Resource

Molecular Cell

Knockout-Rescue Embryonic Stem Cell-Derived Mouse Reveals Circadian-Period Control by Quality and Quantity of CRY1

Graphical Abstract

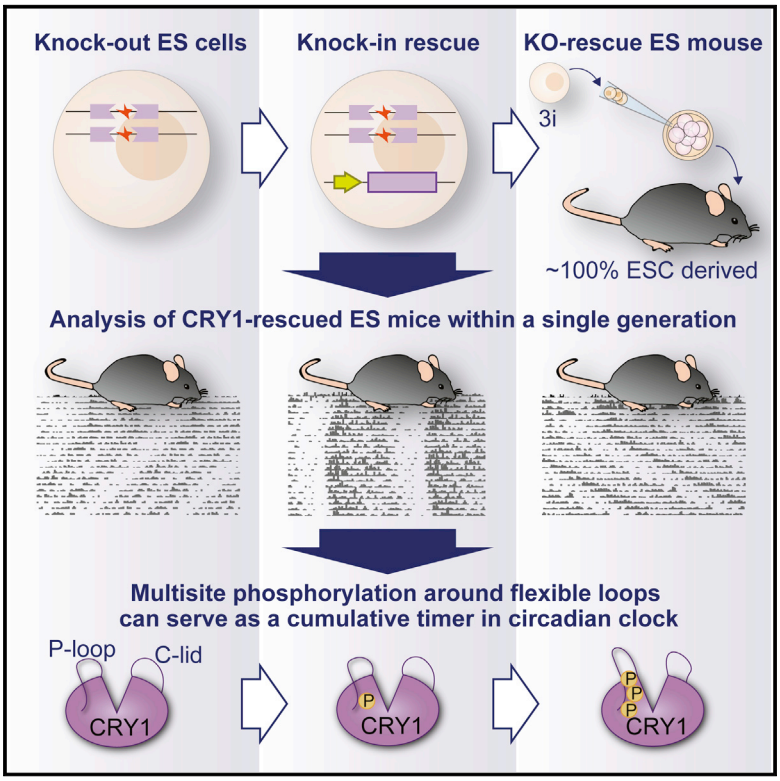

Highlights

- A KO-rescue ES mouse method was developed to produce 20 different KO-rescue strains
- Multisite phosphorylation of CRY1 can serve as a cumulative timer
- CRY1-PER2 interaction confers a robust circadian rhythmicity in mice
- Flexible loops of CRY1 determine circadian period in mice without a turnover change

Authors

Koji L. Ode, Hideki Ukai,
Etsuo A. Susaki, ...,
Masato T. Kanemaki, Hiroshi Kiyonari,
Hiroki R. Ueda

Correspondence

uedah-tky@umin.ac.jp

In Brief

Ode et al. establish an efficient method to conduct gene-rescue experiments in mutant mice. Applying the method to knock in a series of CRY1 mutants into *Cry1*$^{-/-}$:*Cry2*$^{-/-}$ mice, they discover that multisite phosphorylation around the flexible loop domains of CRY1 determine the period length of mammalian circadian clock in vivo.

Ode et al., 2017, Molecular Cell *65*, 1–15
January 5, 2017
http://dx.doi.org/10.1016/j.molcel.2016.11.022

CellPress

Please cite this article in press as: Ode et al., Knockout-Rescue Embryonic Stem Cell-Derived Mouse Reveals Circadian-Period Control by Quality and Quantity of CRY1, Molecular Cell (2016), http://dx.doi.org/10.1016/j.molcel.2016.11.022

Molecular Cell
Resource

Knockout-Rescue Embryonic Stem Cell-Derived Mouse Reveals Circadian-Period Control by Quality and Quantity of CRY1

Koji L. Ode,[1,2,8] Hideki Ukai,[2,8] Etsuo A. Susaki,[1,2,3,8] Ryohei Narumi,[2,9] Katsuhiko Matsumoto,[2] Junko Hara,[2] Naoshi Koide,[2] Takaya Abe,[4] Masato T. Kanemaki,[3,5,6] Hiroshi Kiyonari,[4,7] and Hiroki R. Ueda[1,2,10,*]
[1]Department of Systems Pharmacology, Graduate School of Medicine, The University of Tokyo, 7-3-1 Hongo, Bunkyo-ku, Tokyo 113-0033, Japan
[2]Laboratory for Synthetic Biology, RIKEN Quantitative Biology Center, 1-3 Yamadaoka, Suita, Osaka 565-0871, Japan
[3]PRESTO, Japan Science and Technology Agency (JST), 4-1-8 Honcho, Kawaguchi, Saitama, 332-0012, Japan
[4]Genetic Engineering Team, RIKEN Center for Life Science Technologies, 2-2-3 Minatojima-minamimachi, Chuo-ku, Kobe, Hyogo 650-0047, Japan
[5]Division of Molecular Cell Engineering, National Institute of Genetics, Research Organization of Information and Systems, Yata 1111, Mishima, Shizuoka 411-8540, Japan
[6]Department of Genetics, School of Life Science, SOKENDAI, Mishima, Shizuoka 411-8540, Japan
[7]Animal Resource Development Unit, RIKEN Center for Life Science Technologies, 2-2-3 Minatojima-minamimachi, Chuo-ku, Kobe, Hyogo 650-0047, Japan
[8]Co-first author
[9]Present address: Laboratory of Proteome Research, National Institutes of Biomedical Innovation, Health and Nutrition, Ibaraki, Osaka 567-0085, Japan
[10]Lead Contact
*Correspondence: uedah-tky@umin.ac.jp
http://dx.doi.org/10.1016/j.molcel.2016.11.022

SUMMARY

To conduct comprehensive characterization of molecular properties in organisms, we established an efficient method to produce knockout (KO)-rescue mice within a single generation. We applied this method to produce 20 strains of almost completely embryonic stem cell (ESC)-derived mice ("ES mice") rescued with wild-type and mutant *Cry1* gene under a *Cry1*$^{-/-}$:*Cry2*$^{-/-}$ background. A series of both phosphorylation-mimetic and non-phosphorylation-mimetic CRY1 mutants revealed that multisite phosphorylation of CRY1 can serve as a cumulative timer in the mammalian circadian clock. KO-rescue ES mice also revealed that CRY1-PER2 interaction confers a robust circadian rhythmicity in mice. Surprisingly, in contrast to theoretical predictions from canonical transcription/translation feedback loops, the residues surrounding the flexible P loop and C-lid domains of CRY1 determine circadian period without changing the degradation rate of CRY1. These results suggest that CRY1 determines circadian period through both its degradation-dependent and -independent pathways.

INTRODUCTION

A gene-rescue experiment under mutant background is powerful and has been used in mammalian genetics (Antoch et al., 1997), but the research procedures often require several generations of animal crosses to obtain genetically modified mice. To overcome these problems, it is ideal if one can perform next-generation mammalian genetics, which can be defined as a production and phenotype analysis of genetically modified mice within a single generation. We previously reported that an injection of three-inhibitor (3i)-treated embryonic stem cells (ESCs) into early stage embryos at eight-cell stage can produce chimera mice with efficient contribution of ESC-derived cells (Kiyonari et al., 2010). Using this technique, it will be plausible to analyze the phenotype of gene-rescued mouse within a single generation by using mutant ESCs as a host cell line for the rescued gene.

Among various applications for this technological platform, the mammalian circadian clock is an ideal model system because of its underlying complex and dynamic molecular networks. The E/E'-box-mediated transcriptional program has a critical role in the core autoregulatory loop of the mammalian circadian clock (Mohawk et al., 2012). In this loop, basic helix-loop-helix (bHLH)-PAS (Per-ARNT-Sim) transcription activators such as BMAL1 and CLOCK form heterodimers that bind to E/E'-box *cis*-elements in the promoter regions of their target genes including the *Per* and *Cry* genes; CRYs in turn form repressor complexes including PERs and other binding partners (Brown et al., 2005; Duong et al., 2011; Kim et al., 2015) that physically associate with the BMAL1/CLOCK complex to inhibit E/E'-box-mediated transcription. This delayed feedback repression mediated by CRYs, especially CRY1, plays a pivotal role in the cell autonomous circadian oscillation in mammals (Khan et al., 2012; Ukai-Tadenuma et al., 2011).

This model of transcriptional/translational feedback repression leads to theoretical predictions that the increased turnover rate of transcription repressor mRNAs or proteins results in

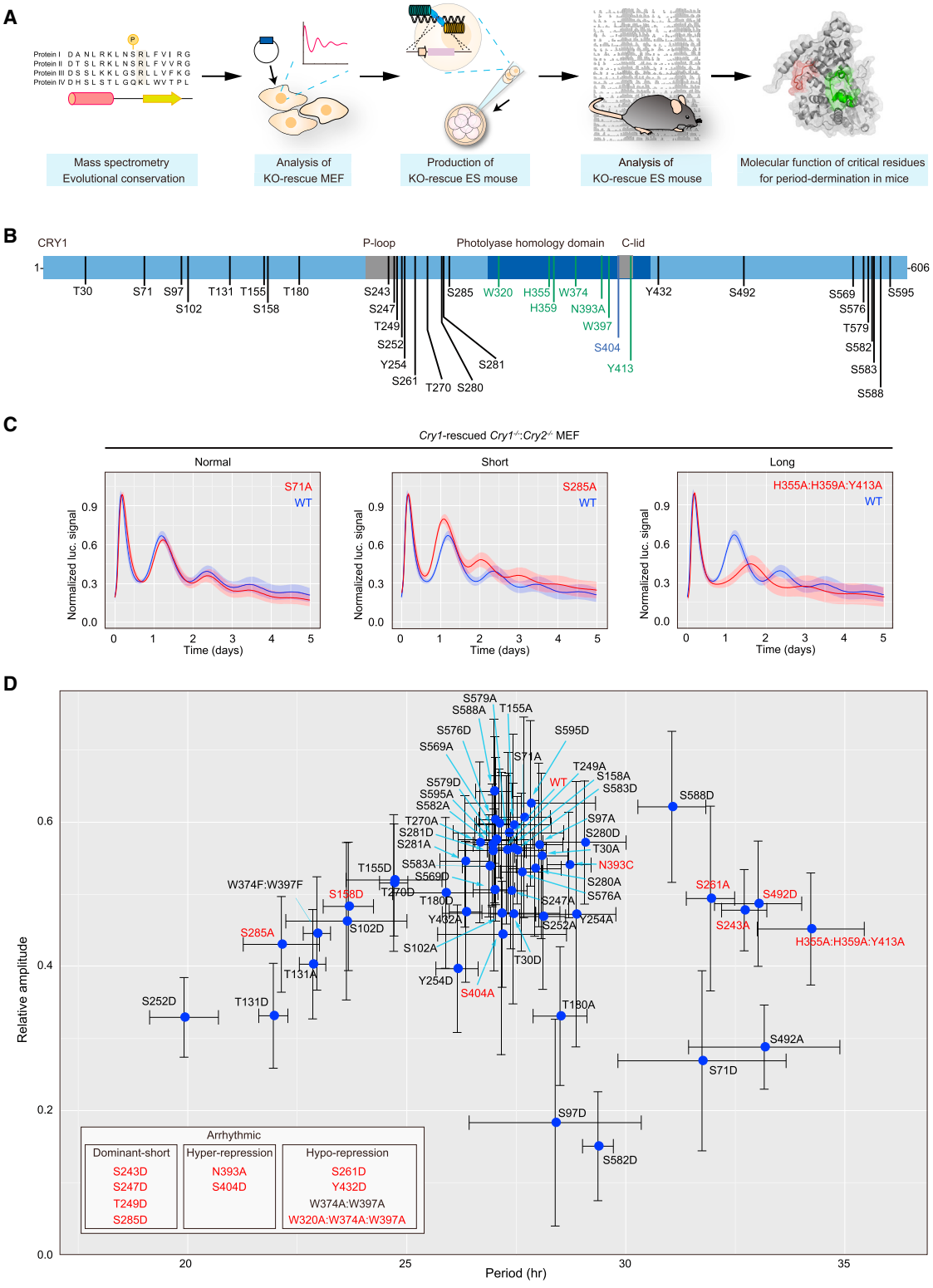

Figure 1. The Phenotype Analysis of KO-Rescue MEFs

(A) A systems framework to reveal the critical residues of CRY1 for controlling the circadian period in vivo.

(B) Identified (black) and predicted (blue) phosphorylation sites, and conserved residues involved in canonical electron-transfer pathway in 6-4 photolyase (green). Identified phosphorylated peptides are shown in Table S1.

(legend continued on next page)

circadian-period shortening (Forger, 2011). Several lines of evidence support this prediction that circadian period of mammalian clocks can be controlled by protein stability of CRY1/2. For example, FBXL3, a component of Skp1-Culin-F-box-protein (SCF) ubiquitin ligase complex that guides CRY1/2 to proteasome-mediated proteolysis, shortens circadian period (Busino et al., 2007; Godinho et al., 2007; Siepka et al., 2007). By contrast, KL001, which binds to the flavin adenine dinucleotide (FAD)-binding pocket of CRY1/2 and stabilizes the protein, lengthens the circadian period (Hirota et al., 2012; Nangle et al., 2013).

However, there are some results that contradict with the theoretical prediction. For example, destabilization of CRY1 by AMPK-dependent phosphorylation should results in the shortening of circadian period, but stimulation of AMPK results in period lengthening (Lamia et al., 2009). A recent chemical-biology study even succeeded to synthesize a compound bound to the CRY1/2 FAD-binding pocket, that shortens the circadian period, but surprisingly, stabilizes CRY1 (Oshima et al., 2015). These results imply that the stability-independent period determination of circadian clocks, demonstrated in other organisms (Larrondo et al., 2015; Nakajima et al., 2005), might be also true for mammalian circadian clocks.

In this study, we established an efficient method to produce knockout (KO)-rescue mice within a single generation (KO-rescue ES mouse method) by the 3i-8-cell method. We then applied this method to the production of 20 strains of different *Cry1* wild-type/mutants knockin mice under a $Cry1^{-/-}$:$Cry2^{-/-}$ double mutant background. The mutagenesis of CRY1 revealed that residues surround the flexible P loop and C-lid domains of CRY1 determine the period length of circadian clock, and most of them have only a marginal effect on the degradation rate of CRY1, suggesting the presence of period determination mechanism independent of CRY1's degradation rate. This high-throughput knockin mouse strategy would accelerate circadian and other fields of biology using various mouse strains harboring modified genes or reporters and thus may help to shift the conventional way of mammalian genetics, which depends largely on the crossing of animals.

RESULTS

The Phenotype Analysis of KO-Rescue Mouse Embryonic Fibroblasts

We intended to analyze complex and dynamic molecular networks in organisms by focusing on CRY1 protein in mammalian circadian clocks as a model system (Figure 1A). The first step is the identification of critical residues of CRY1 for circadian-period determination. Phospho-peptides derived from CRY1-overexpressed 293T cells were analyzed with mass spectrometer (Figure S1A). We identified 27 phosphorylation sites (Figure 1B; Table S1) including previously reported residues targeted by mitogen-activated protein kinase (MAPK S247) (Sanada et al., 2004), AMPK (S71 and S280) (Lamia et al., 2009), and DNA-PK (S588) (Gao et al., 2013). We did not identify phosphorylation at S404 but included this residue as a possible phosphorylation site based on database prediction as a protein kinase C (PKC)-targeted site (Lamia et al., 2009). Three groups of potential functional residues in CRY1 (tryptophan triplet W320, W374, and W397; histidine/tyrosine triplet H355, H359, and Y413; and asparagine N393) were also selected based on a canonical electron-transfer pathway proposed in its evolutionally most-related protein, 6-4 photolyase (Figure S1B) (Ozturk et al., 2007; Sancar, 2004).

Each phosphorylated residue was then mutated to phosphorylation-mimetic aspartic acid (D) or non-phosphorylation-mimetic alanine (A). The conserved electron-transfer motifs were mutated to alanine. The mutant CRY1 was then expressed in $Cry1^{-/-}$:$Cry2^{-/-}$ mouse embryonic fibroblast (MEF) under the control of *Cry1* promoter combined with intronic enhancer Rev-Erb/ROR-binding element (RREs) (Ukai-Tadenuma et al., 2011). The expressed CRY1 rescued circadian rhythmicity in the MEF with various period and amplitude depending on the mutations (Figure 1C). A numbers of mutants failed to rescue the detectable rhythmicity; we noticed that there are three classes of these arrhythmic mutants, namely, dominant-short, hyperrepression, and hyporepression types (Figure 1D). Each class of mutant affected the circadian rhythmicity in a qualitatively different manner when it was overexpressed in wild-type NIH 3T3 cells (Figure S1C). When wild-type CRY1 was overexpressed in NIH 3T3 cells, the expression greatly suppressed the amplitude of E-box driven reporter without affecting the period length. Arrhythmic hyporepression mutants failed to suppress the amplitude suggesting the reduced transcription-repressor activity. In contrast, mutants classified as arrhythmic hyperrepression further suppressed the amplitude compared with wild-type CRY1, suggesting the enhanced transcription-repression activity. Unlike these classes, arrhythmic dominant-short mutants accelerated the speed of circadian oscillation when they were overexpressed in NIH 3T3 cells. We interpreted that intrinsic period of these arrhythmic dominant-short mutants are extremely short.

The overall in vitro phenotype results are summarized in Figure 1D and Table S2. Although mutation on the conserved electron-transfer motifs caused different effects, we expect that these motifs in mammalian cryptochrome may not have an electron transfer activity, at least in the regulation of circadian rhythmicity, because phenylalanine substitution of tryptophan (W374F:W397F) (23.0 ± 0.3 hr) or cysteine substitution of

(C) Examples of circadian oscillation in $Cry1^{-/-}$:$Cry2^{-/-}$ MEF monitored by transiently transfected reporter plasmid expressing destabilized luciferase driven by *Per2* gene's promoter (P(*Per2*)-d*Luc*). For the $Cry1^{-/-}$:$Cry2^{-/-}$ MEF rescue experiments in this and the other figures, the luciferase signal was normalized such that the maximum value of each time course data is one, and shown as average (solid line) ± SD (shade). Note that the same data for wild-type rescue was shown in each panel for comparison.

(D) Period and amplitude of rescued circadian rhythmicity in $Cry1^{-/-}$:$Cry2^{-/-}$ MEF was calculated for each mutant CRY1, and shown as average ± SD. The arrhythmic mutants were classified based the experiments using NIH 3T3 cells as shown in Figure S1C. The value of period and relative amplitude, and number of experiments are shown in Table S2. Wild-type/mutant CRY1 indicated in red were used for KO-rescue ES mouse experiment in Figures 4 and 5.

See also Tables S1 and S2 and Figure S1.

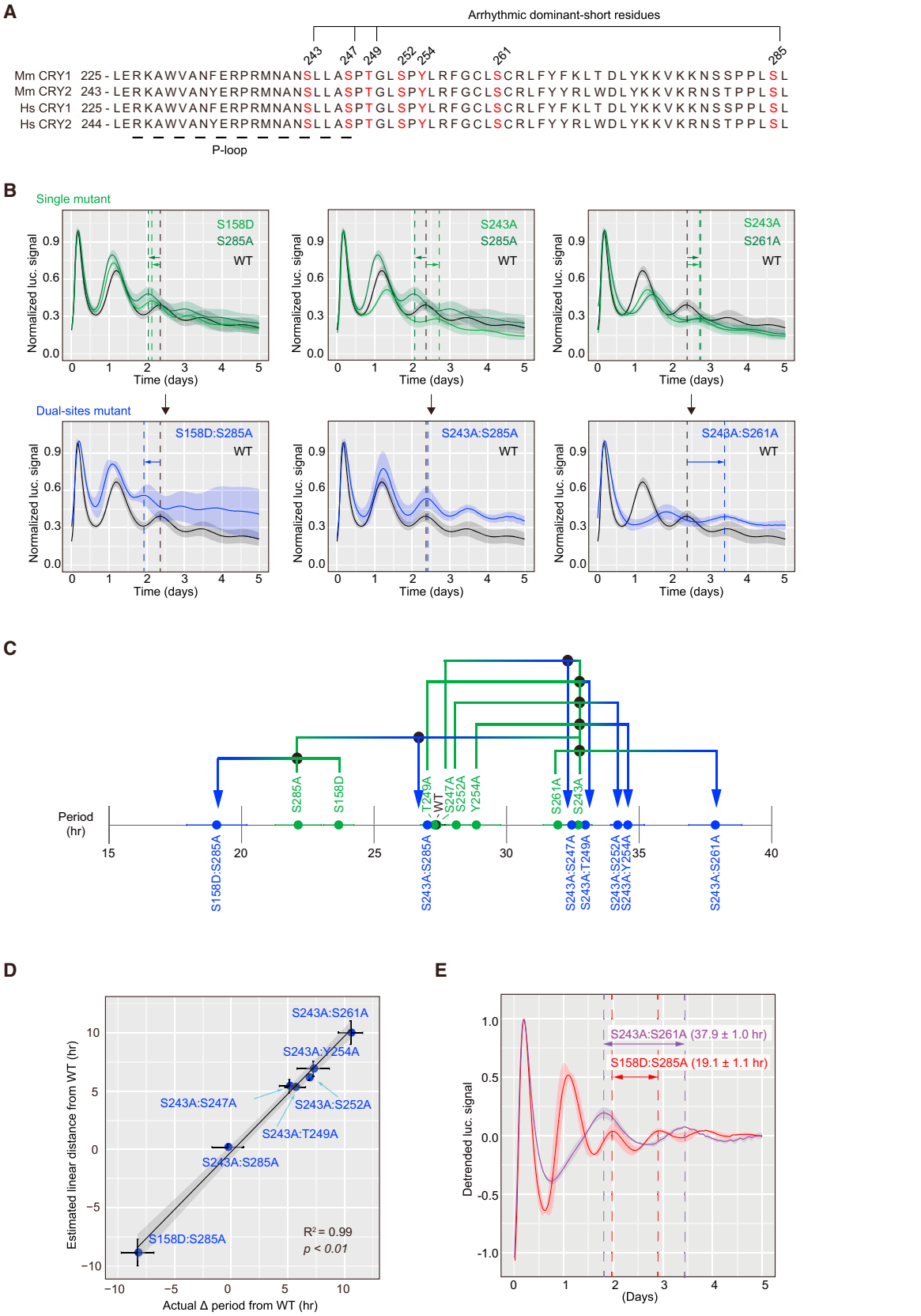

(legend on next page)

asparagine N393C (corresponds to insect-specific cryptochromes) (28.7 ± 0.5 hr) support robust circadian oscillations. Many of phosphorylation-mimetic mutation on the phosphorylation cluster near the P loop domain greatly shorten the circadian rhythmicity (e.g., S243D, S247D, T249D, S252D, and S285D). Among all analyzed phosphorylation residues, S243 appears to be the most critical residue for period determination because this site is the only residue that has bidirectional effects on circadian period when mutated to A or D.

Multisite Phosphorylation of CRY1 Can Serve as a Cumulative Timer

We then asked the logic behind the period determination, especially focusing on the phosphorylation cluster near the P loop domain (Figure 2A). If the serial phosphorylation events are triggered by priming phosphorylation at the specific site, then the priming site works as a "switch" and governs the others. In this case, alanine mutation on the priming phosphorylation site is epistatic to the alanine mutation of the other residues. In contrast, if the accumulation of local negative charge additively evokes the response, then the effects of alanine mutations can be cumulative, working as a "timer." To distinguish these scenarios, we introduced two alanine mutations for a various pair of phosphorylation sites indicated in Figure 2A. We also included one phosphorylation-mimetic mutant (S158D) outside of the region near the P loop domain.

The period of every analyzed CRY1 with mutations in two phosphorylation residues revealed clear additive relationship on the period determination (Figure 2B). The additive rule was applicable not only to the distant pairs of residues (i.e., S158D and S285A) but also to local pairs within the restricted area near the P loop (Figures 2C and 2D; Table S3). This assay also revealed the highly flexible nature of CRY1-dependent period determination at nearly 2-fold dynamic range (Figure 2E). These results suggest that multisite phosphorylation of CRY1 serves as a cumulative timer in mammalian circadian clock.

Because S243 was the only residue that had both shortening and lengthening effects on period, we investigated what kinase is responsible for the phosphorylation at S243. Several algorithms for kinase prediction listed casein kinase I (CKI) as a potential kinase to phosphorylate S243 or downstream S247 (Table S4). Furthermore, we found that one of the responsible kinase for S243 phosphorylation, at least in 293T cells, is CKIδ/ε, a major kinase that accelerates the pace of circadian oscillation (Figure S2A; Table S5) (Mohawk et al., 2012).

S243 is conserved in mammalian CRY proteins and plant 6-4 photolyases but is rarely conserved among the other proteins in cryptochrome superfamily (Figure S2B). Phylogeny analysis revealed that serine/threonine and negatively charged aspartic acid and glutamic acid reciprocally emerge among the area surrounding S243 position (Figures S2B–S2D). A phylogenetic theory suggests that phosphorylation activating the protein function tends to be aspartic acid or glutamic acid in the ancestral form (Pearlman et al., 2011). Applying this rationale to mammalian CRY proteins, mammalian cryptochromes for the circadian clock might interchange the static negative charge of D/E with a dynamic phosphorylation site for controlling circadian period.

The Development of a KO-Rescue ES Mouse Method

To directly confirm the in vivo significance of period-determining residues identified in *Cry1*-rescue assay in *Cry1*$^{-/-}$:*Cry2*$^{-/-}$ MEF, we next conducted *Cry1*-rescue assay under *Cry1*$^{-/-}$:*Cry2*$^{-/-}$ mice. The coat color of *Cry1*$^{-/-}$:*Cry2*$^{-/-}$ ES mice was almost identical with the original *Cry1*$^{-/-}$:*Cry2*$^{-/-}$ mice, suggesting the contamination of host embryo cells, which would result in white coat color, was negligible (Figure 3A). PCR-based genotyping further confirmed that the contamination of cells from the host embryo having a wild-type *Cry2* allele was no more than 0.001% (Figure 3A). Both original *Cry1*$^{-/-}$:*Cry2*$^{-/-}$ mice and the double-knockout ES mice had arrhythmic behavior (Figure 3B). We then knocked in *Cry1* under the control of *Cry1* promoter including an intronic RRE element (Ukai-Tadenuma et al., 2011) into the ROSA26 locus (Figure 3C; Table S6). During the series of knockin targeting, we used not only a conventional targeting method with on-feeder ESC culture but also a more efficient targeting method with feeder-free ESC culture and TALENs (transcription activator-like effector nucleases) (Figures S3A–S3F) (Sung et al., 2013). These gene-targeting conditions are specified in Table S7.

The *Cry1* cassette introduced in ROSA26 locus rescued circadian rhythmicity in their behavior with slightly different periods depending on the direction of insertion (Figures 3D and 3F; Table S7). We chose the cassette designed to be inserted to ROSA26 locus in antisense direction for subsequent analyses, because their behavioral period in ES mice with a single antisense cassette (24.2-24.3 hr) was closer to the free-running periods of *Cry1*$^{+/-}$;*Cry2*$^{-/-}$ mice (24.29 hr) (van der Horst et al., 1999). The stringency of the *Cry1* KO-rescue ES mouse method was confirmed by the following two experiments. First, circadian rhythmicity was not observed if *Cry1* gene is driven by

Figure 2. Multisite Phosphorylation of CRY1 Can Serve as a Cumulative Timer

(A) Sequence alignment of P loop and downstream sequence. Indicated residues were used in double mutants in this figure. Mm: *Mus musculus*. Hs: *Homo sapiens*.

(B) Example of circadian period of wild-type (black), or mutant CRY1 with single (green) or double (blue) phosphorylation residues. The experiment was carried out as in Figure 1. Note that the data of wild-type and of single site mutants (green) were identical data shown in Figures 1C and 1D.

(C) The rescued period lengths for indicated combination of dual-sites mutants were calculated. Note that the periods of single site mutants (green) were identical data shown in Figure 1D.

(D) The effect of double mutants to circadian period is the sum of the effect of individual single mutations. The x axis is the period of rescued *Cry1*$^{-/-}$:*Cry2*$^{-/-}$ MEF rescued by indicated double mutants as shown in (C). The y axis is the estimated period by adding the period difference between wild-type and individual point mutants. The period lengths are shown as average ± SD and summarized in Table S3.

(E) Circadian oscillation of CRY1 double mutant showing shortest period (S158D:S285A) and longest period (S243A:S261A). The experiment was carried out as Figure 1, and detrended luciferase signal are shown as average ± SD.

See also Tables S3, S4, and S5 and Figure S2.

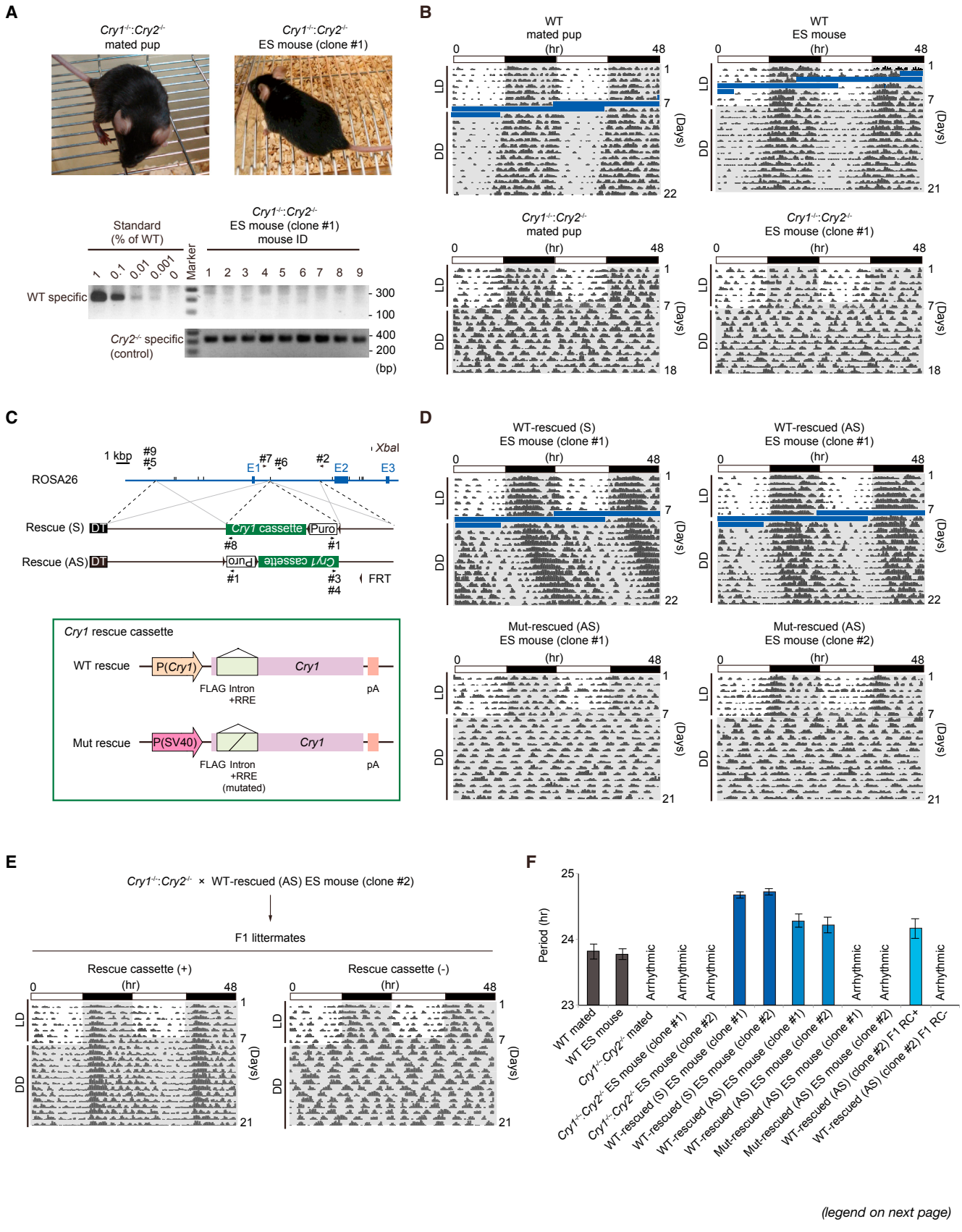

(legend on next page)

non-circadian promoter (Figures 3C and 3D, Mut rescue) (Ukai-Tadenuma et al., 2011). Second, F1 littermates of rescued mice and *Cry1*$^{-/-}$:*Cry2*$^{-/-}$ mice showed circadian rhythmicity only if the offspring had *Cry1*-knocked-in allele in the ROSA26 locus (Figure 3E). These results indicate that the behavioral rhythmicity is induced by the *Cry1*-rescue cassette. Note that, for the "Mut rescue" condition, we did not analyze the exact reason of arrhythmicity; it may be due to the altered periodicity for the expression timing of *Cry1* or the altered expression level of *Cry1*. In the following experiments, we used the same (wild-type [WT]) promoter to compare the phenotypes of different *Cry1* mutants.

The Phenotype Analysis of KO-Rescue ES Mice

Seventeen *Cry1* mutants (see Figure 1D, red colored mutants) were selected for the assay of *Cry1*-rescue ES mice. The normal-period mutants in MEFs (N393C and S404A) had almost identical or shorter period in ES mice (24.2 ± 0.1 and 23.9 ± 0.1 hr, respectively) compared with the circadian period of WT-rescued ES mice (24.2 ± 0.1 hr) (Figure 4A). The short-period mutants in MEFs (S158D and S285A) had shorter circadian period in ES mice (23.9 ± 0.1 hr and 23.8 ± 0.1 hr, respectively) (Figure 4B). In contrast, long-period mutants in MEFs (S243A, S492D, and HHY) had significantly longer circadian period in ES mice (24.6 ± 0.05, 25.4 ± 0.1, and 26.6 ± 0.3 hr) (Figure 4C).

The arrhythmic dominant-short mutants in MEFs (S243D, S247D, T249D, and S285D) rescued the circadian rhythmicity in KO-rescue ES mice and exhibited markedly shorter period (21.1 ± 0.1, 22.4 ± 0.1, 22.7 ± 0.1, and 22.7 ± 0.1 hr, respectively) (Figure 4D). These results strongly suggest that the intrinsic periods of arrhythmic dominant-short mutants are markedly shorter than that of any other rhythmic mutants in MEFs. In addition, all three arrhythmic hyporepression mutants (S261D, Y432D, and WWW) in MEFs also had arrhythmic phenotype in mice (Figure 4E). These results further strengthen the conclusion that arrhythmic hyporepression mutants are the loss-of-function form of protein and are qualitatively different from arrhythmic dominant-short mutants.

Correlation between the Circadian Phenotype of KO-Rescue MEFs and ES Mice

Overall, KO-rescue ES mice results summarized in Figure 5A demonstrates a striking correlation between circadian periods observed in MEFs and those observed in KO-rescue ES mice. Note that the magnitude of circadian-period alteration in each CRY1 mutant ES mice from the wild-type was smaller than that of CRY1 mutant MEFs, converging close to 24 hr in KO-rescue ES mice (Figure 5B).

There are several mutants, the phenotypes of which in ES mice are not in line with those of MEFs; S261A mutant had long-period phenotype in MEFs whereas the mutant ES mice had an arrhythmic phenotype (Figure 5C). In addition, the phenotypes of N393A and S404D mutant both of which had arrhythmic hyperrepression phenotypes in MEFs were not reproduced in ES mice: N393A mutant ES mice had a long-period phenotype (25.0 ± 0.4 hr) (Figure 5D), whereas the period of S404D tends to be short in the first 2 weeks after the entry to constant darkness condition and then became longer in the next 2 weeks (Figure 5E). Interestingly, we found that all CRY1 mutants with arrhythmic (S261A, S261D, Y432D, and WWW) or unstable-period (S404D) phenotypes in ES mice had a significant reduction in the interaction with PER2 when these CRY1 mutants were expressed in 293T cells and quantified for the amount of PER2 co-immunoprecipitated with CRY1 (Figure 5F). These results highlight the importance of CRY1-PER2 interaction in stable rhythmicity in vivo.

Correlation of CRY1 Turnover Rate and Circadian Period

To investigate what biochemical properties of CRY1 protein can determine the circadian period and amplitude, we analyzed CRY1's degradation rate (Figure S4A) and transcription-repression activity (Figure S4B). As a result, significant correlation was observed between CRY1 half-life and circadian period and between CRY1 repression activity and circadian amplitude but not for other combinations (Figure S4C). These results are consistent with the canonical relationship between CRY1 degradation and circadian period (Forger, 2011) and between CRY1 repression activity and circadian amplitude (Khan et al., 2012).

To our surprise, a number of mutants had altered circadian period without significant changes in protein half-life (Figure 6A, red circles). Of note, a group of long period mutants (HHY, S492D, S492A, and S243A) had no significant change in protein stability, but their period was significantly longer than the most stable mutant S588D (Gao et al., 2013). Also, it is notable that the arrhythmic dominant-short mutants (S243D, S247D,

Figure 3. The Development of a KO-Rescue ES Mouse Method

(A) 3i-cultured *Cry1*$^{-/-}$:*Cry2*$^{-/-}$ ESCs were derived from B6-backcrossed *Cry1*$^{-/-}$:*Cry2*$^{-/-}$ strain (van der Horst et al., 1999). ESC clones producing male ES mouse with black coat color were selected. Contamination of host embryo cells was evaluated by semiquantitative genomic PCR for *Cry2* locus with primers specific to wild-type or *Cry2*$^{-/-}$ allele.

(B) Representative actograms of mated pups (wild-type or *Cry1*$^{-/-}$:*Cry2*$^{-/-}$ C57BL/6) and ES mice derived from ESCs of wild-type or *Cry1*$^{-/-}$:*Cry2*$^{-/-}$ C57BL/6. Shaded regions indicate dark phase. Time windows marked as blue line indicate system shutdown due to the electric outage of the mouse facility.

(C) A structure of *Cry1*-rescue cassette and targeted ROSA26 locus. "WT rescue" cassette drives *Cry1* expression by promoter of *Cry1* gene and intronic RRE element (Ukai-Tadenuma et al., 2011). In the "Mut rescue" cassette, the promoter is swapped to SV40 promoter and the sequences of intronic RRE are mutated. Arrows with numbers indicate PCR primers for ESC screenings and genome integrity confirmations, summarized in Table S6. AS, antisense, pA, poly-A tail; S, sense.

(D) Representative actograms of *Cry1*$^{-/-}$:*Cry2*$^{-/-}$ ES mice rescued with WT rescue cassette in sense (S) or antisense (AS) direction, and Mut rescue cassette in antisense (AS) direction.

(E) Representative actograms of F1 offspring obtained by crossing the rescued ES mice with *Cry1*$^{-/-}$:*Cry2*$^{-/-}$ strain. The offspring harboring the *Cry1*-rescue cassette (indicated as "+") at the ROSA26 locus showed circadian behavioral rhythmicity.

(F) Summary of the quantified period of circadian behavioral rhythmicity shown as average ± SD (during DD condition). The period lengths and gene-targeting conditions are summarized in Table S7.

See also Tables S6 and S7 and Figure S3.

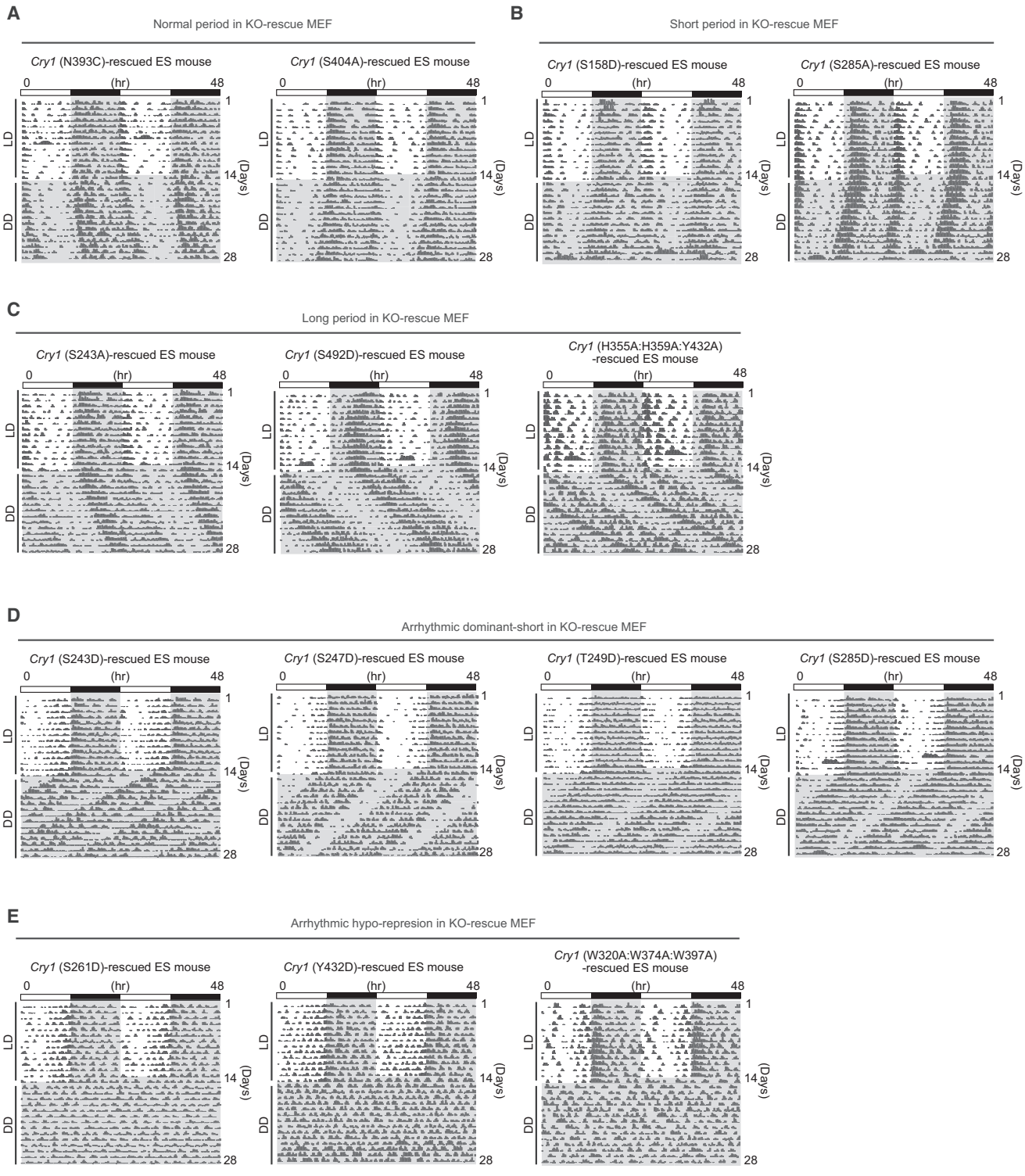

Figure 4. The Phenotype Analysis of KO-Rescue ES Mice

Representative actograms of a *Cry1*$^{-/-}$:*Cry2*$^{-/-}$ mouse rescued with indicated mutant *Cry1* in anti-sense direction, exhibiting near-wild-type period length (A), shorter period length (B), longer period (C), arrhythmic dominant-short phenotype (D), or arrhythmic hyporepression phenotype (E) in *Cry1*$^{-/-}$:*Cry2*$^{-/-}$ MEF rescue experiment shown in Figure 1. All mutant CRY1-rescued ES mouse lines analyzed in this study except for mutants shown in Figures 5C–5E are shown. The period lengths and gene-targeting conditions are summarized in Table S7.

See also Table S7.

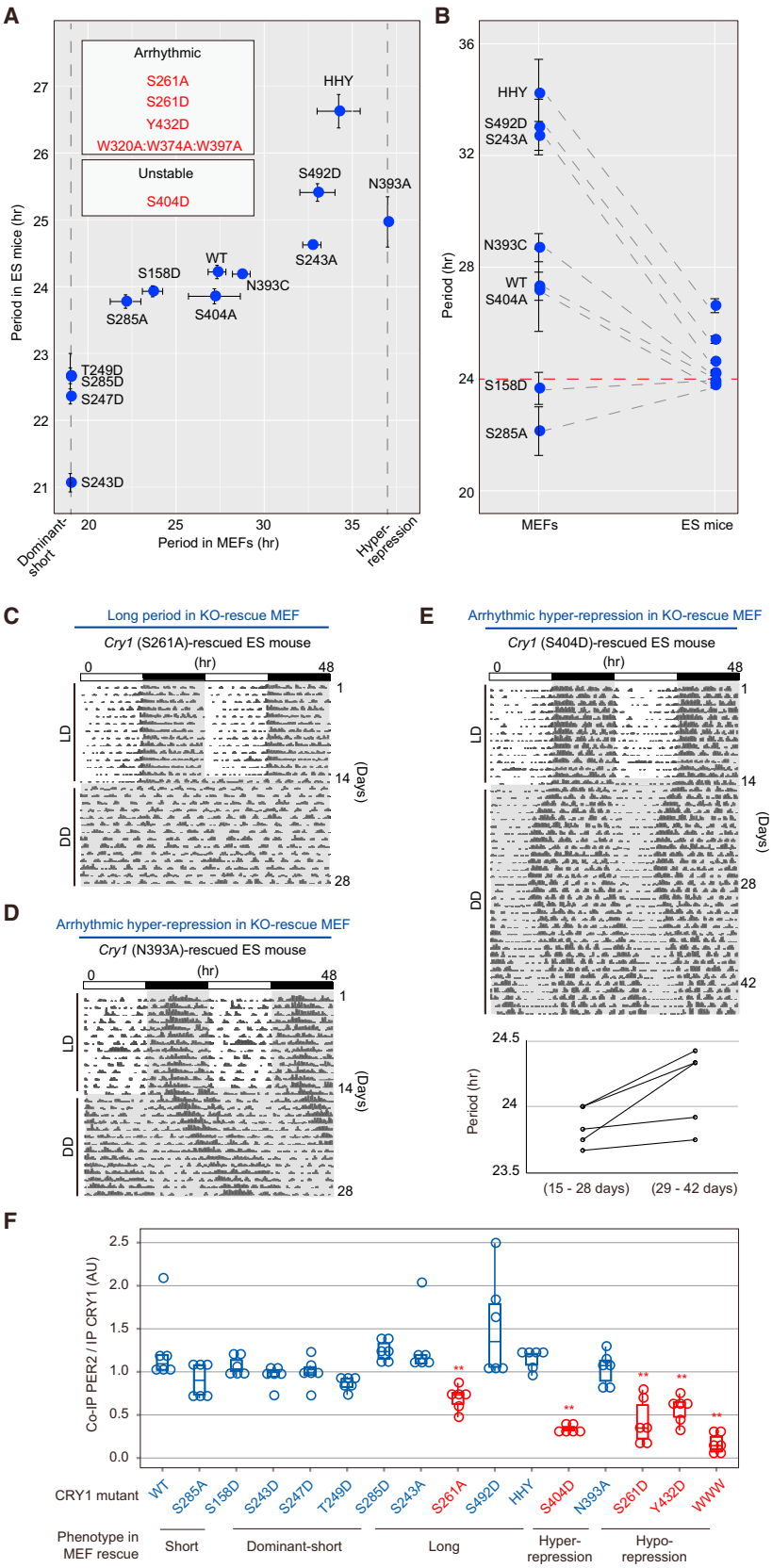

Figure 5. The Circadian Phenotype of KO-Rescue ES Mice

(A) Summary of period in behavioral rhythmicity. The representative behavioral plots are shown in Figure 4 and Figures 5B–5D. The behavioral period in constant darkness condition was calculated and shown as average ± SD. The period (or, categories in arrhythmic mutants) of molecular oscillation recorded in rescued MEF (i.e., results shown in Figure 1D) is plotted against the period of behavioral rhythmicity in rescued mice. Mutants shown in red are arrhythmic or show unstable period in rescued mice.

(B) For each mutant that was rhythmic both in rescued MEF and rescued mice, the period lengths of MEF and mice were compared.

(C) A representative actogram of a *Cry1*$^{-/-}$:*Cry2*$^{-/-}$ mouse rescued with S261A mutant CRY1.

(D) A representative actogram of a *Cry1*$^{-/-}$:*Cry2*$^{-/-}$ mouse rescued with N393A mutant CRY1.

(E) Top: a representative actogram of a *Cry1*$^{-/-}$:*Cry2*$^{-/-}$ mouse rescued with S404D mutant CRY1. Because the period lengths of behavioral rhythmicity are unstable in this mutant line, the recoding was extended over 4 weeks in constant darkness. Bottom: the period was calculated for the first 2 weeks and the second 2 weeks of constant darkness condition for each S404D-rescued mouse.

(F) Interaction of CRY1 mutant and PER2 was quantified by co-immunoprecipitation (IP) and mass spectrometry-based quantification. Three different PER2-derived peptides were quantified in two independent experiments. Data are shown as box-and-whisker plot and individual quantified values; each circle indicates the quantified value of peptide derived from PER2 protein normalized by the amount of CRY1 protein.

**$p < 0.05$; $p > 0.1$, Student's t test compared with WT. See also Table S7.

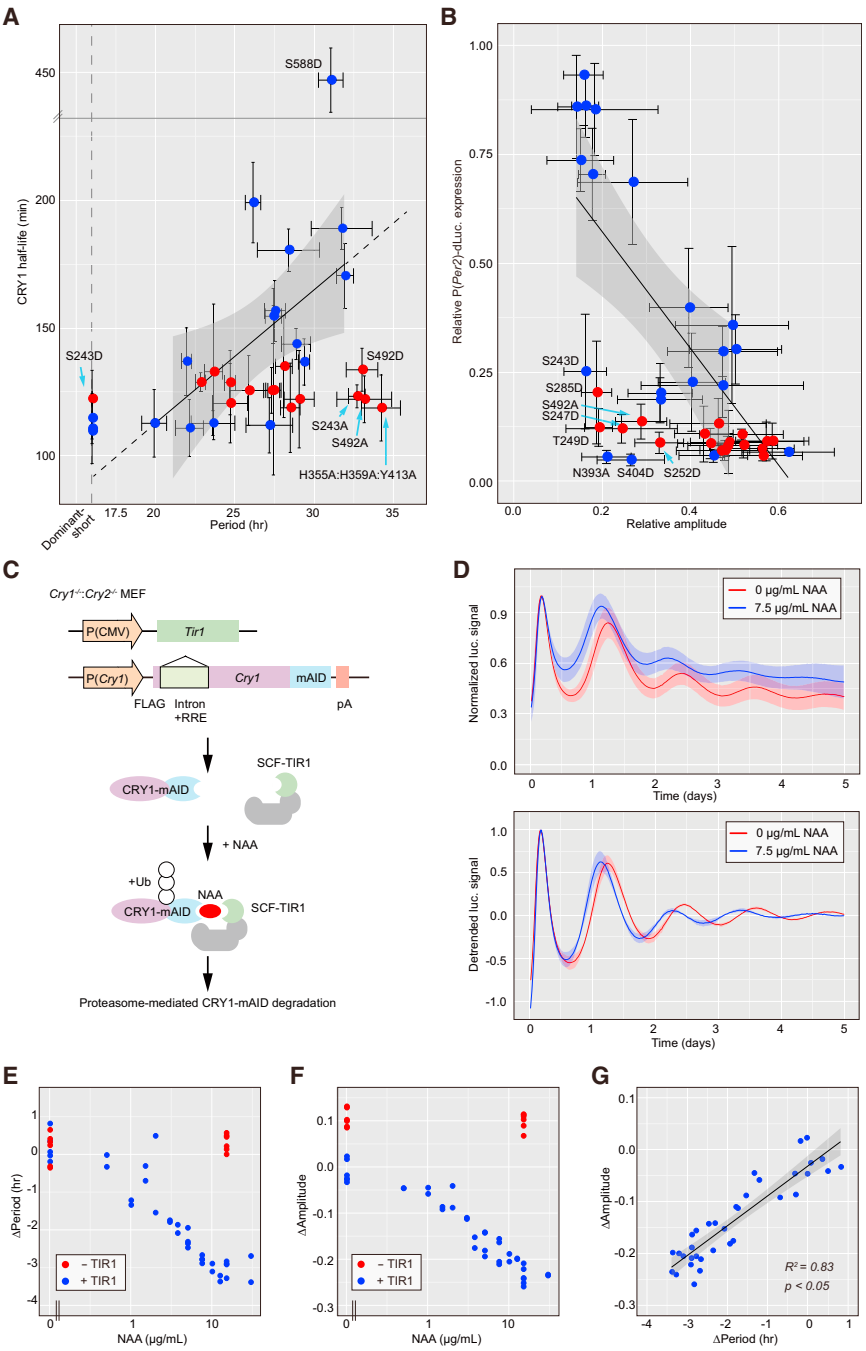

Figure 6. Causality of Increased CRY1 Turnover Rate to Circadian Period Shortening

(A) Circadian period of each mutant CRY1 in rescued MEF (data shown in Figure 1D) was plotted against protein half-life (average ± SD). Mutants with significantly shorter or longer half-life ($p < 0.1$, Student's t test compared with wild-type) are shown in blue, and mutants with similar half-life compared with wild-type are shown in red. "Arrhythmic hyper-repression" mutants were not plotted. See Figure S4A for the half-life of each mutants and Figure S4C for the linear regression.

(B) Relative amplitude of circadian rhythmicity in rescued MEF (data shown in Figure 1D) was plotted against relative activity of P(*Per2*)-d*Luc* co-transfected with each mutant CRY1 (average ± SD). Mutants with significantly higher or lower repression activity ($p < 0.1$, Student's t test compared with wild-type) are shown in blue, and mutants with similar repression activity compared with wild-type are shown in red. See Figure S4B for the half-life of each mutants and Figure S4C for the linear regression.

(C) Scheme of the construction of CRY1-mAID system. *Tir1* was expressed under constitutive (non-circadian) promoter. A fragment of the original AID/IAA17 tag called mini-AID (mAID) (Kubota et al., 2013) was fused with the C-terminal of CRY1. AID-tagged *Cry1* was expressed under the Cry1-rescue promoter. Addition of NAA induces the degradation of AID-tagged CRY1. Ub, ubiquitin.

(D) Circadian oscillation of rescued MEF with AID-tagged CRY1 in the presence of TIR1. The experiments were carried out as in Figure 1 except for that indicated amount of NAA was added to the medium. The upper half shows the normalized signal of P(*Per2*)-d*Luc* signal, and the lower half is the detrended oscillation signal.

(E) Changes in the oscillation period of CRY1-mAID rescued MEF. The period length of each experiment was compared with the average period of CRY1-mAID rescued MEF in the presence of TIR and 0 μg/mL of NAA.

(F) Changes in the oscillation amplitude of CRY1-mAID rescued MEF. The relative amplitude of each experiment was compared with the average amplitude of CRY1-mAID rescued MEF in the presence of TIR and 0 μg/mL of NAA.

(G) Correlation of amplitude reduction and period shortening by induction of CRY1-mAID degradation.

See also Figure S4.

T249D, and S285D) had decreased protein stability, if any, similar to the other short mutants. Hence, it is difficult to quantitatively explain the remarkable period shortening observed in ES mice only by decreased CRY1 protein stability.

Causality of Increased CRY1 Turnover Rate to Circadian Period Shortening

The finding of mutants that alter the circadian period with modest effect on the CRY1 stability challenges the canonical relationship between CRY1 degradation and period shortening. To ask the causality between them, we tried to induce targeted and artificial proteolysis of CRY1 by using Auxin-induced degradation (AID) system (Figure 6C) (Kubota et al., 2013; Nishimura et al., 2009): the AID-tag is recognized by TIR1 protein, a subunit of SCF ubiquitin ligase, in the presence of auxin, leading to the proteasome-mediated degradation of AID-tagged protein in an auxin's dose-dependent manner. The tagged CRY1 successfully repressed the E-box-mediated transcription and that activity is reduced by the addition of synthetic auxin (naphthaleneacetic acid [NAA]) in a dose-dependent and TIR-dependent manner

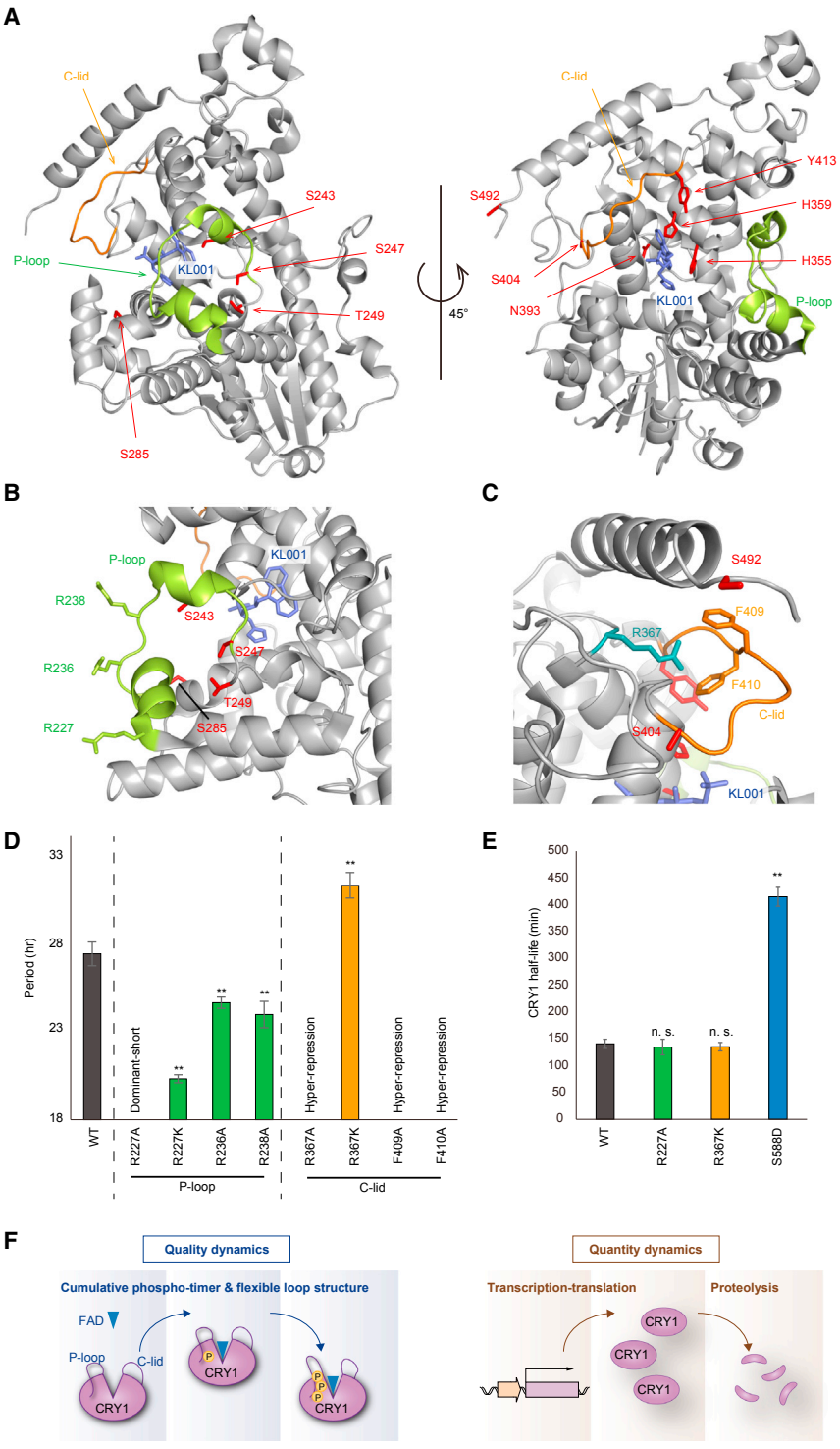

Figure 7. P Loop and C-lid as Period-Determining Domains of CRY1 Protein

(A) Crystal structure of Mm CRY2 bound to FAD analog KL001 (PDB: 4MLP) (Nangle et al., 2013). Note that S404 is not conserved in Mm CRY2 (substituted with alanine).

(B) A close-up view of the P loop and surrounding regions.

(C) A close-up view of the C-lid and surrounding regions. Two phenylalanine residues (F409, F410) on the C-lid are sterically close to an R367 residue that penetrates into the C-lid loop structure.

(D) Circadian period lengths of indicated CRY1 mutants. The arrhythmic mutants were classified based on the phenotype of NIH 3T3 overexpressed with the mutant (shown in Figure S5F). The experiments were carried out as in Figure 1.

**$p < 0.05$; Student's t test compared with WT. The period lengths are shown as average ± SD and summarized in Table S8.

(E) Protein half-life of indicated CRY1 mutants shown as average ± SD. The experiments were carried out as in Figure 6. **$p < 0.05$, n.s. $p > 0.1$; Student's t test compared with WT.

(F) Proteolysis-dependent and -independent circadian-period determination by CRY1.

See also Table S8 and Figures S5 and S6.

(Figures S4D–S4F). Furthermore, tagged CRY1 rescued the circadian rhythmicity in the *Cry1*$^{-/-}$:*Cry2*$^{-/-}$ MEF (Figure 6D). The period of rescued rhythmicity became shorter in a NAA-dose-dependent manner (Figures 6D and 6E), confirming the causal effect of CRY1 degradation on circadian period shortening. The amplitude of oscillating reporter signal was also decreased by the induction of CRY1 proteolysis (Figure 6F), resulting in a linear correlation between period and amplitude (Figure 6G). The result of induced CRY1 degradation suggest that the canonical relationships between circadian period and CRY1's half-life is applicable to circadian phenotype several CRY1 mutants, although such relationships cannot explain some exceptional mutants with drastic effects on the circadian period and rhythmicity.

P Loop and C-lid as Period-Determining Domains of CRY1 Protein

We then mapped the positions of such exceptional mutation on the reported CRY structures. Note that CRY2 structure bound with KL001 was used in this structural analysis because P loop structure was determined only in CRY2 but not in CRY1 (Nangle et al., 2013). Residue position number corresponding to CRY1 was used because of the consistency with our mutagenesis assay. We focused on residues that, when mutated, result in markedly long-period phenotypes (HHY, S492D, S492A, and S243A), arrhythmic dominant-short phenotypes (S243D, S247D, T249D, and S285D) or arrhythmic hyperrepression phenotypes (S404D and N393A). Figure 7A indicates that all the above-listed residues are located around

the co-factor (FAD/KL001) binding pocket of the CRY protein, especially the two loop domain called the P loop and C-lid. H355, H359, and Y413 are located near the co-factor (FAD/KL001) binding pocket and can interact with a potential co-factor. Consistently, KL001 had no detectable effect on HHY mutant (Figure S5A). Although S492 has no direct interaction with C-lid domain or co-factor binding pocket, phosphorylation of S492 residue might affect the structure of downstream, non-crystalized C-terminal domain. On the basis of these arrangement of non-canonical period-determining residues, we anticipated that the P loop and C-lid, both of which are suggested to be flexible domain (Figure S5B) (Czarna et al., 2013; Nangle et al., 2013, 2014; Schmalen et al., 2014; Xing et al., 2013), are the core domains of CRY1 in circadian-period determination. If these domains are responsible for period determination without changing CRY1 protein stability, it may be possible that structure-guided engineering of CRY1 mutation on these domain structures recapitulates proteolysis-independent period modulation.

To test this, we focused on the arginine triplet on the P loop domain (i.e., R227, R236, and R238) (Figures 7B and S5C) because the positively charged and surface-oriented arginine triplet may be involved in the interaction between CRY1 and other factors. We also focused on R367 and F409/F410 for C-lid structure because the interaction of these residues may restrict the flexibility of the C-lid (Figures 7C and S5D). As expected, mutation on each residue altered circadian oscillation of CRY1-rescued *Cry1*$^{-/-}$:*Cry2*$^{-/-}$ MEF (Figure 7D). The alanine substitution of each arginine triplet resulted in a short-period phenotype with most drastic effect for the R227A mutation. The arrhythmic dominant-short phenotype of R227A was partially attenuated when the positively charged residue lysine substituted the position (R227K). In contrast, alanine substitution of the F409 and F410 at C-lid and the same substitution of their contact partner R367 resulted in arrhythmic hyper-repression phenotype (Figures 7D, S5E, and S5F; Table S8). When lysine substituted the R367 position, the R367K mutant had a significantly longer phenotype. We then picked up R227A and R367K mutants for P loop and C-lid domain, respectively, and investigated the protein stability of these mutants. As expected, Figure 7E shows that the protein stability of these mutants was not significantly changed compared with wild-type. The longer half-life of S588D mutant as observed in Figure 6A confirmed the robustness of this assay. The involvement of FAD-binding pocket and surrounding regions in the period determination are also supported by the result showing that cysteine residues involved in the disulfide bond at C-lid terminal (Schmalen et al., 2014) and residues mutated in *Drosophila* CRY (*cry*^{b}) (Stanewsky et al., 1998) are also important for the circadian-period determination in mammalian CRY1 (Figures S6B and S6C). Taken together, these data suggest that structural/electrostatic properties of P loop and C-lid are important for proteolysis-independent circadian-period determination (Figure 7F).

DISCUSSION

Multisite Phosphorylation of CRY1 Can Serve as a Cumulative Timer

The linear and additive effect of phosphorylation mutants (Figure 2) implies that CRY1 plays a role as a cumulative timer. Previous studies as well as database/algorithm-based prediction provide (Table S4) various possible kinases responsible for the phosphorylation of CRY1. The multisite phosphorylation may integrate internal information (e.g., spent time) and external information (e.g., environmental signals) and converts them into circadian-period modulation. Indeed, we identified dual phosphorylated peptide near the flexible P loop (Table S1, S243/S247). Multisite phosphorylation often occurs and regulates flexible structures or intrinsically disordered regions. This type of regulation was found in FRQ in *Neurospora* and PER in mammals (Wright and Dyson, 2015) and may be a shared design principle for the control of circadian time keeping mechanism.

The role of phosphorylation may be different depending on the target site; in our assay, S243 is the only residue, of which phosphorylation-mimetic and non-phosphorylation-mimetic mutants have opposite effect in period length, suggesting that proper level of phosphorylation on this site and/or a timely phosphorylation along with the circadian cycle is important for the circadian time keeping. There are other classes of phosphorylation site, in which only either the phosphorylation-mimetic or the non-phosphorylation-mimetic mutant had a significant effect on the circadian period (e.g., S71). This may be related to the phosphorylation level of each site. If one site is constitutively phosphorylated during the circadian cycle, then non-phosphorylation-mimetic mutation rather than phosphorylation-mimetic one would cause a severe effect. Contrary, if one site is rarely phosphorylated, then phosphorylation-mimetic mutation may cause a greater effect. For the mutants showing that both of alanine and aspartic acid substitution cause the similar effect on period length (e.g., T131), it is likely that the exact composition of side chain as well as negative charge might be important for the circadian phenotype. To validate these predictions in future studies, quantitative measurement of phosphorylation at each site, efficient detection of multi-phosphorylated peptides, and identification of responsible kinases/phosphatases will be important.

CRY1-PER2 Interaction Confers a Robust Circadian Rhythmicity in Mice

Previous study indicated that disulfide bond between C363 and C412 residues in CRY1 controls CRY1's affinity to PER2 protein, and mutation on either one of two cysteine residues increased the CRY1-PER2 interaction (Schmalen et al., 2014). However, our study showed that C363A mutation resulted in period lengthening while C412A mutation resulted in period shortening (Figure S6B). Thus, the phenotype of circadian period appears to be not matched with the phenotype of CRY1-PER2 interaction. This suggests that the phenotype of circadian period is caused by altered structure of mutated residues not simply by the breakage of disulfide bond. This result also implies that the importance of CRY1-PER2 interaction for circadian clockworks may lie in aspects other than period-determination processes. Notably, our KO-rescue ES mouse analyses revealed the role of CRY1-PER2 interaction for the robust circadian rhythmicity in vivo rather than period-determination and CRY1's repression activity (Figure 5).

Convergence of Period Length toward 24 hr in Mice

It has been reported that period variance of SCN and organism behavior is smaller than that of MEFs and dispersed SCN cells (Liu et al., 2007; Welsh et al., 2004). Our KO-rescue ES mouse analyses further revealed that period difference of CRY1 mutants observed in MEFs converged toward 24 hr in ES mice (Figure 5B). It is difficult to attribute the conversion effect to *Cry1*-driven feedback loop because we created long and short period mutants, all of which directly targeted the CRY1 molecule. Despite this, the periods of short mutants measured in MEFs were lengthened in ES mice, and the periods of long mutants measured in MEFs were shortened in ES mice. Thus, it is suggested that the molecular/cellular nature of convergence-to-24 hr-effect, not just the reduction of variance, is not related to *Cry1* gene. Interestingly, Ono et al. demonstrated that circadian oscillation can be observed in *Cry1*$^{-/-}$:*Cry2*$^{-/-}$ mice in a limited developmental condition (Ono et al., 2013), suggesting the presence of *Cry1*/*2*-independent circadian oscillator. Our CRY1 mutagenesis assay revealed that CRY1-PER2 interaction is particularly important for robust rhythmicity in mice. Phosphorylation of PER2 by CKIδ/ε have several intriguing features such as temperature-compensation (Isojima et al., 2009) and reciprocal regulation of CKIε (Qin et al., 2015) that have a potential to create phosphorylation-based autonomous oscillators (Jolley et al., 2012). These features imply that part of the mammalian circadian rhythmicity might rely upon *Per2*-driven oscillators. Therefore, one possible perspective is that *Per2*-driven oscillator couples with *Cry1*-driven oscillator to confer a near 24-hr rhythmicity.

Circadian-Period Determination by CRY1 Degradation-Dependent and -Independent Mechanisms

Our study suggests that the P loop and C-lid are responsible for the protein-stability-independent period determination. Previous studies revealed that C-lid forms an interface between CRY1/2 and PER2 (Figure S6D) (Nangle et al., 2014; Schmalen et al., 2014) or FBXL3 (Xing et al., 2013), and the C-lid structure is affected by the binding of these proteins (Figure S6E). P loop is not directly involved in the interface between PER2 or FBXL3, but it may affect the interaction through creating the co-factor binding pocket. Indeed, residues of CRY1 affecting the interaction with PER2 identified in this study locate around co-factor binding pocket (hence surrounding C-lid or P loop) (Figure S6D). However, our study suggests that the period-determination mechanism can be independent from CRY1 stability that is regulated through FBXL3 and PER2 competition. Thus, it is also possible that the C-lid and P loop may regulate circadian period through the interaction with other proteins because CRY proteins function in a 2-MDa complex composed of tens of proteins (Brown et al., 2005; Duong et al., 2011; Kim et al., 2015). In summary, this study proposes that mammalian circadian period is controlled not only by the turnover rate of CRY1, a behavior determined by the *quantity* of molecules, but also by the *quality* of each molecule characterized by the structure of flexible loops and phosphorylation status.

EXPERIMENTAL PROCEDURES

Detailed information was described in Supplemental Experimental Procedures.

Circadian Reporter Assay using *Cry1*$^{-/-}$:*Cry2*$^{-/-}$ MEFs and NIH 3T3 Cells

Real-time monitoring of circadian reporter using culture cells was performed as previously described (Ukai-Tadenuma et al., 2011). In brief, cells were transfected with pGL3-P(*Per2*)-d*Luc* reporter plasmid and each *Cry1* gene expression vector. The cells were synchronized by adding forskolin to the medium. The bioluminescence was monitored at 30°C.

Generation of ES Mice and Behavior Analysis

An ESC clone was injected into 8-cell-stage ICR embryos to generate ES mice (Kiyonari et al., 2010). C57BL/6 wild-type mice (9 weeks old), *Cry1*$^{-/-}$:*Cry2*$^{-/-}$ mice (12 weeks old), ES mice (7-10 weeks old), F1 animals of WT rescue (AS) (10 weeks old) were entrained to a light-12 hr:dark-12 hr cycle for at least 2 weeks and then the locomotor activity was collected in the light-dark condition for 1-2 weeks and then in the dark-dark (DD) condition for another 2-4 weeks. All experimental procedures and housing conditions involving animals and their care were approved the Institutional Animal Care and Use Committee of RIKEN Kobe Branch.

Analysis of CRY1 Half-Life and Transcription-Repression Activity

Vector construct that express *Cry1*::*luciferase* under the non-circadian CMV promoter (pMU2-*Cry1*::*luciferase*) was transfected to *Cry1*$^{-/-}$:*Cry2*$^{-/-}$ MEFs. Luciferase signal was chased after the addition of 400 μg/mL of cycloheximide to the medium. Transcription repression assay was performed as described previously (Khan et al., 2012).

SUPPLEMENTAL INFORMATION

Supplemental Information includes Supplemental Experimental Procedures, six figures, and eight tables and can be found with this article online at http://dx.doi.org/10.1016/j.molcel.2016.11.022.

AUTHOR CONTRIBUTIONS

H.R.U., K.L.O., H.U., and E.A.S. designed the study. K.L.O performed most of the cellular/biochemical experiments, and data analysis. H.U., E.A.S., N.K., T.A., and H.K. established a KO-rescue ES mouse method. E.A.S and J.H. performed animal experiments. R.N. and K.M. performed phospho-peptide quantification. M.T.K. and K.L.O. established the AID system in circadian assay. H.R.U., K.L.O., H.U., and E.A.S. wrote the manuscript. All authors discussed the results and commented on the manuscript.

ACKNOWLEDGMENTS

We thank all the lab members at RIKEN QBiC and the University of Tokyo, in particular, Dr. Masahiro Hayashi and Dr. Genshiro A. Sunagawa for helping with animal experiments; Chikako Imai, Ayumi Kishimoto, Satoko Morino, and Marie Muramatsu for their effort to maintain ESCs; Junko Garçon, Kaori Yamanaka, and Shino Hirahara for their effort with the production of ES mice; Maki Ukai-Tadenuma for helping with the cellular assay; Dr. Rikuhiro G. Yamada for assisting mice behavior analysis; and Yoshiki Nagashima for supporting analyses with a mass spectrometer. We also thank the LARGE, RIKEN CLST for housing the mice. We thank Dr. Arthur Millius for critical reading and valuable comments on the manuscript. We are grateful to Dr. Eisuke Nishida for providing pcDNA3-*Myc-mPer2* and Dr. Haruhiko Takisawa for sharing unpublished data. This work was supported by a grant from AMED-CREST (H.R.U.), CREST (H.R.U.), Brain/MINDS (H.R.U.), Basic Science and Platform Technology Program for Innovative Biological Medicine (H.R.U.), the Cell Innovation Program (H.R.U), KAKENHI Grants-in-Aid from JSPS (Scientific Research S, 25221004, H.R.U.; Scientific Research on Innovative Areas, 23115006, H.R.U.; Young Scientists B, 25830146, K.L.O.; Challenging Exploratory Research, 16K14653, K.L.O.; Young Scientists A, 15H05650, E.A.S.), the strategic programs for R&D of RIKEN (H.R.U.), an intramural Grant-in-Aid from the RIKEN QBiC (H.R.U.), grants from Takeda Science Foundation

(H.R.U. and E.A.S.), the RIKEN Special Postdoctoral Research Program (E.A.S.), a Grant-in-Aid by PRESTO from JST (E.A.S.), a Grant-in-Aid from the Japan Foundation for Applied Enzymology (E.A.S.), and a grant of the Brain Sciences Project of the Center for Novel Science Initiatives of the National Institutes of Natural Sciences (BS281004, E.A.S.).

Received: September 14, 2016
Revised: October 24, 2016
Accepted: November 15, 2016
Published: December 22, 2016

REFERENCES

Antoch, M.P., Song, E.J., Chang, A.M., Vitaterna, M.H., Zhao, Y., Wilsbacher, L.D., Sangoram, A.M., King, D.P., Pinto, L.H., and Takahashi, J.S. (1997). Functional identification of the mouse circadian Clock gene by transgenic BAC rescue. Cell *89*, 655–667.

Brown, S.A., Ripperger, J., Kadener, S., Fleury-Olela, F., Vilbois, F., Rosbash, M., and Schibler, U. (2005). PERIOD1-associated proteins modulate the negative limb of the mammalian circadian oscillator. Science *308*, 693–696.

Busino, L., Bassermann, F., Maiolica, A., Lee, C., Nolan, P.M., Godinho, S.I., Draetta, G.F., and Pagano, M. (2007). SCFFbxl3 controls the oscillation of the circadian clock by directing the degradation of cryptochrome proteins. Science *316*, 900–904.

Czarna, A., Berndt, A., Singh, H.R., Grudziecki, A., Ladurner, A.G., Timinszky, G., Kramer, A., and Wolf, E. (2013). Structures of *Drosophila* cryptochrome and mouse cryptochrome1 provide insight into circadian function. Cell *153*, 1394–1405.

Duong, H.A., Robles, M.S., Knutti, D., and Weitz, C.J. (2011). A molecular mechanism for circadian clock negative feedback. Science *332*, 1436–1439.

Forger, D.B. (2011). Signal processing in cellular clocks. Proc. Natl. Acad. Sci. USA *108*, 4281–4285.

Gao, P., Yoo, S.H., Lee, K.J., Rosensweig, C., Takahashi, J.S., Chen, B.P., and Green, C.B. (2013). Phosphorylation of the cryptochrome 1 C-terminal tail regulates circadian period length. J. Biol. Chem. *288*, 35277–35286.

Godinho, S.I., Maywood, E.S., Shaw, L., Tucci, V., Barnard, A.R., Busino, L., Pagano, M., Kendall, R., Quwailid, M.M., Romero, M.R., et al. (2007). The after-hours mutant reveals a role for Fbxl3 in determining mammalian circadian period. Science *316*, 897–900.

Hirota, T., Lee, J.W., St John, P.C., Sawa, M., Iwaisako, K., Noguchi, T., Pongsawakul, P.Y., Sonntag, T., Welsh, D.K., Brenner, D.A., et al. (2012). Identification of small molecule activators of cryptochrome. Science *337*, 1094–1097.

Isojima, Y., Nakajima, M., Ukai, H., Fujishima, H., Yamada, R.G., Masumoto, K.H., Kiuchi, R., Ishida, M., Ukai-Tadenuma, M., Minami, Y., et al. (2009). CKIε/δ-dependent phosphorylation is a temperature-insensitive, period-determining process in the mammalian circadian clock. Proc. Natl. Acad. Sci. USA *106*, 15744–15749.

Jolley, C.C., Ode, K.L., and Ueda, H.R. (2012). A design principle for a post-translational biochemical oscillator. Cell Rep. *2*, 938–950.

Khan, S.K., Xu, H., Ukai-Tadenuma, M., Burton, B., Wang, Y., Ueda, H.R., and Liu, A.C. (2012). Identification of a novel cryptochrome differentiating domain required for feedback repression in circadian clock function. J. Biol. Chem. *287*, 25917–25926.

Kim, J.Y., Kwak, P.B., Gebert, M., Duong, H.A., and Weitz, C.J. (2015). Purification and analysis of PERIOD protein complexes of the mammalian circadian clock. Methods Enzymol. *551*, 197–210.

Kiyonari, H., Kaneko, M., Abe, S., and Aizawa, S. (2010). Three inhibitors of FGF receptor, ERK, and GSK3 establishes germline-competent embryonic stem cells of C57BL/6N mouse strain with high efficiency and stability. Genesis *48*, 317–327.

Kubota, T., Nishimura, K., Kanemaki, M.T., and Donaldson, A.D. (2013). The Elg1 replication factor C-like complex functions in PCNA unloading during DNA replication. Mol. Cell *50*, 273–280.

Lamia, K.A., Sachdeva, U.M., DiTacchio, L., Williams, E.C., Alvarez, J.G., Egan, D.F., Vasquez, D.S., Juguilon, H., Panda, S., Shaw, R.J., et al. (2009). AMPK regulates the circadian clock by cryptochrome phosphorylation and degradation. Science *326*, 437–440.

Larrondo, L.F., Olivares-Yañez, C., Baker, C.L., Loros, J.J., and Dunlap, J.C. (2015). Circadian rhythms. Decoupling circadian clock protein turnover from circadian period determination. Science *347*, 1257277.

Liu, A.C., Welsh, D.K., Ko, C.H., Tran, H.G., Zhang, E.E., Priest, A.A., Buhr, E.D., Singer, O., Meeker, K., Verma, I.M., et al. (2007). Intercellular coupling confers robustness against mutations in the SCN circadian clock network. Cell *129*, 605–616.

Mohawk, J.A., Green, C.B., and Takahashi, J.S. (2012). Central and peripheral circadian clocks in mammals. Annu. Rev. Neurosci. *35*, 445–462.

Nakajima, M., Imai, K., Ito, H., Nishiwaki, T., Murayama, Y., Iwasaki, H., Oyama, T., and Kondo, T. (2005). Reconstitution of circadian oscillation of cyanobacterial KaiC phosphorylation in vitro. Science *308*, 414–415.

Nangle, S., Xing, W., and Zheng, N. (2013). Crystal structure of mammalian cryptochrome in complex with a small molecule competitor of its ubiquitin ligase. Cell Res. *23*, 1417–1419.

Nangle, S.N., Rosensweig, C., Koike, N., Tei, H., Takahashi, J.S., Green, C.B., and Zheng, N. (2014). Molecular assembly of the period-cryptochrome circadian transcriptional repressor complex. eLife *3*, e03674.

Nishimura, K., Fukagawa, T., Takisawa, H., Kakimoto, T., and Kanemaki, M. (2009). An auxin-based degron system for the rapid depletion of proteins in nonplant cells. Nat. Methods *6*, 917–922.

Ono, D., Honma, S., and Honma, K. (2013). Cryptochromes are critical for the development of coherent circadian rhythms in the mouse suprachiasmatic nucleus. Nat. Commun. *4*, 1666.

Oshima, T., Yamanaka, I., Kumar, A., Yamaguchi, J., Nishiwaki-Ohkawa, T., Muto, K., Kawamura, R., Hirota, T., Yagita, K., Irle, S., et al. (2015). C-H activation generates period-shortening molecules that target cryptochrome in the mammalian circadian clock. Angew. Chem. Int. Ed. Engl. *54*, 7193–7197.

Ozturk, N., Song, S.H., Ozgür, S., Selby, C.P., Morrison, L., Partch, C., Zhong, D., and Sancar, A. (2007). Structure and function of animal cryptochromes. Cold Spring Harb. Symp. Quant. Biol. *72*, 119–131.

Pearlman, S.M., Serber, Z., and Ferrell, J.E., Jr. (2011). A mechanism for the evolution of phosphorylation sites. Cell *147*, 934–946.

Qin, X., Mori, T., Zhang, Y., and Johnson, C.H. (2015). PER2 differentially regulates clock phosphorylation versus transcription by reciprocal switching of CK1ε activity. J. Biol. Rhythms *30*, 206–216.

Sanada, K., Harada, Y., Sakai, M., Todo, T., and Fukada, Y. (2004). Serine phosphorylation of mCRY1 and mCRY2 by mitogen-activated protein kinase. Genes Cells *9*, 697–708.

Sancar, A. (2004). Regulation of the mammalian circadian clock by cryptochrome. J. Biol. Chem. *279*, 34079–34082.

Schmalen, I., Reischl, S., Wallach, T., Klemz, R., Grudziecki, A., Prabu, J.R., Benda, C., Kramer, A., and Wolf, E. (2014). Interaction of circadian clock proteins CRY1 and PER2 is modulated by zinc binding and disulfide bond formation. Cell *157*, 1203–1215.

Siepka, S.M., Yoo, S.H., Park, J., Song, W., Kumar, V., Hu, Y., Lee, C., and Takahashi, J.S. (2007). Circadian mutant Overtime reveals F-box protein FBXL3 regulation of cryptochrome and period gene expression. Cell *129*, 1011–1023.

Stanewsky, R., Kaneko, M., Emery, P., Beretta, B., Wager-Smith, K., Kay, S.A., Rosbash, M., and Hall, J.C. (1998). The cryb mutation identifies cryptochrome as a circadian photoreceptor in *Drosophila*. Cell *95*, 681–692.

Sung, Y.H., Baek, I.J., Kim, D.H., Jeon, J., Lee, J., Lee, K., Jeong, D., Kim, J.S., and Lee, H.W. (2013). Knockout mice created by TALEN-mediated gene targeting. Nat. Biotechnol. *31*, 23–24.

Ukai-Tadenuma, M., Yamada, R.G., Xu, H., Ripperger, J.A., Liu, A.C., and Ueda, H.R. (2011). Delay in feedback repression by cryptochrome 1 is required for circadian clock function. Cell *144*, 268–281.

van der Horst, G.T., Muijtjens, M., Kobayashi, K., Takano, R., Kanno, S., Takao, M., de Wit, J., Verkerk, A., Eker, A.P., van Leenen, D., et al. (1999). Mammalian Cry1 and Cry2 are essential for maintenance of circadian rhythms. Nature *398*, 627–630.

Welsh, D.K., Yoo, S.H., Liu, A.C., Takahashi, J.S., and Kay, S.A. (2004). Bioluminescence imaging of individual fibroblasts reveals persistent, independently phased circadian rhythms of clock gene expression. Curr. Biol. *14*, 2289–2295.

Wright, P.E., and Dyson, H.J. (2015). Intrinsically disordered proteins in cellular signalling and regulation. Nat. Rev. Mol. Cell Biol. *16*, 18–29.

Xing, W., Busino, L., Hinds, T.R., Marionni, S.T., Saifee, N.H., Bush, M.F., Pagano, M., and Zheng, N. (2013). SCF(FBXL3) ubiquitin ligase targets cryptochromes at their cofactor pocket. Nature *496*, 64–68.